

Accepted Manuscript

Synthesis, characterisation and antimicrobial activity of copper(II) complexes with hydrazone derived from 3-hydroxy-5-(hydroxymethyl)-2-methylpyridine-4-carbaldehyde

Reka-Ştefana Mezey, István Máthé, Sergiu Shova, Maria-Nicoleta Grecu, Tudor Roşu

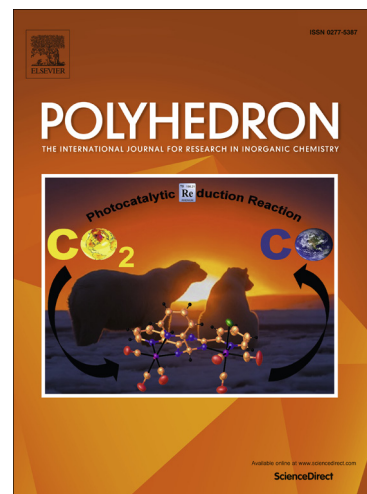
PII: S0277-5387(15)00616-6
DOI: <http://dx.doi.org/10.1016/j.poly.2015.10.035>
Reference: POLY 11620

To appear in: *Polyhedron*

Received Date: 12 July 2015
Accepted Date: 22 October 2015

Please cite this article as: R. Mezey, I. Máthé, S. Shova, M-N. Grecu, T. Roşu, Synthesis, characterisation and antimicrobial activity of copper(II) complexes with hydrazone derived from 3-hydroxy-5-(hydroxymethyl)-2-methylpyridine-4-carbaldehyde, *Polyhedron* (2015), doi: <http://dx.doi.org/10.1016/j.poly.2015.10.035>

This is a PDF file of an unedited manuscript that has been accepted for publication. As a service to our customers we are providing this early version of the manuscript. The manuscript will undergo copyediting, typesetting, and review of the resulting proof before it is published in its final form. Please note that during the production process errors may be discovered which could affect the content, and all legal disclaimers that apply to the journal pertain.



Synthesis, characterisation and antimicrobial activity of copper(II) complexes with hydrazone derived from 3-hydroxy-5-(hydroxymethyl)-2-methylpyridine-4-carbaldehyde

Reka-Ştefana Mezey^{a*}, István Máthé^b, Sergiu Shova^c, Maria-Nicoleta Grecu^d, Tudor Roşu^a

^aDepartment of Inorganic Chemistry, Faculty of Chemistry, University of Bucharest, 23 Dumbrava Rosie, 050107 Bucharest, Romania

^bDepartment of Bioengineering, Faculty of Technical and Social Sciences, Sapientia Hungarian University of Transylvania, Libertatii Square 1, 530104, Miercurea Ciuc, Romania

^cInstitute of Macromolecular Chemistry "Petru Poni", 41A Grigore Ghica Voda, 400786 Iasi, Romania

^dNational Institute of Materials Physics, 077125 Măgurele-Ilfov, Romania

Keywords: copper(II) complexes, pyridoxal isonicotinoyl hydrazone, crystal structure, antimicrobial activity

ABSTRACT

Pyridoxal isonicotinoyl hydrazone (**HL**) and its copper(II) complexes: [CuLCl(H₂O)₂] (**1**), [CuL(OAc)](H₂O) (**2**), [CuL(OAcac)] (**3**), [CuL(NO₃)](H₂O) (**4**), [CuL₂](H₂O) (**5**) were synthesized and characterized. The ligand has been obtained by condensation of 3-hydroxy-5-(hydroxymethyl)-2-methylpyridine-4-carbaldehyde (pyridoxal) hydrochloride with isonicotinoyl hydrazide.

The characterization of the formed compounds was done by ¹H NMR, ¹³C NMR, UV–Vis, IR and EPR spectroscopy as well by thermal studies and elemental analysis. The crystal structure of **HL** has been determined by single crystal X-ray diffraction studies. The microbiological effect of the ligand and all five complexes against both Gram-positive and Gram-negative strains, *Staphylococcus aureus* ATCC 6538, *Bacillus cereus* ATCC 14579, *Escherichia coli* W3110 and *Pseudomonas aeruginosa* ATCC 9027 was tested.

1. Introduction

During the past decay significant researches concerning the metal complexes of hydrazone-type ligands have been undertaken. Especially the hydrazones containing a pyridine ring moiety are of great interest due to their extended applicability in biology and pharmacology as anticonvulsant, antimicrobial, antitubercular, antitumor and analgesic agents [1-5]. Due to their coordination potential to different metal ions and their remarkable versatility, such compounds attracted the interest of the inorganic and bioinorganic chemists as well. Different metal complexes of hydrazone-type ligands were synthesized and proven to possess a wide range of application in catalysis, optic and luminescence field and of course in medicine [6-11].

One of the most interesting class of complexes with hydrazone ligands is the one derived from isonicotinic acid hydrazide. Isonicotinoyl hydrazide, also known as isoniazid, have been largely used as an antimicrobial agent, especially in the treatment of tuberculosis caused by the bacteria *Mycobacterium tuberculosis* [12a, 12b, 12c]. Also, the hydrazones obtained by condensation of isoniazid with various carbonilic compounds have been proven to exhibit antimicrobial effect which in some case was superior to the one of the original hydrazide [13-15]. Further,

the resulting hydrazone can be used as ligand in various complexes structures, the structure of the final coordination compound depending mainly on the number and position of the donor atoms in the molecule. Moreover, some Ni(II), Co(II), Mn (II) complexes have been shown to exhibit enhanced microbiological activity compared to the original ligands [9,11a].

3-hydroxy-5-(hydroxymethyl)-2-methylpyridine-4-carbaldehyde (pyridoxal) is one of the five naturally interconvertible forms of vitamin B₆ [16]. The reason for choosing pyridoxal as derivative agent of isoniazid is linked to its recognized physiological effect as agent influencing the aminoacids metabolism, antioxidant compound and coenzyme involved in numerous metabolic processes [17-20]. Moreover, it was reported that the introduction of the pyridoxal moiety in an azomethine compounds represents a major factor in the synthesis of therapeutic agents [21-23]. On the other hand, pyridoxal isonicotinoyl hydrazone is an interesting reagent for the design of metal complexes, acting as a tridentat ligand. Pyridoxal isonicotinoyl hydrazone was synthesized and reported in previous literature materials [24] but in its unsolvated form.

This paper is a continuation of our previous research and it describes the synthesis and characterization of new complexes of Cu(II) with the hydrazone (Scheme. 1) obtained by the condensation of 3-hydroxy-5-(hydroxymethyl)-2-methylpyridine-4-carbaldehyde with isonicotinoyl hydrazide. Additionally, the crystal structure of the ligand has been studied by X-ray diffraction. The ligand and complexes were tested *in vitro* for their antibacterial activity against both Gram-positive and Gram-negative strains like *Staphylococcus aureus* ATCC 6538, *Bacillus cereus* ATCC 14579, *Escherichia coli* W3110 and *Pseudomonas aeruginosa* ATCC 9027.

2. Experimental

2.1. Materials

Pyridoxal hydrochloride (Sigma) and isonicotinoyl hydrazide (Sigma) were used as purchased without any pre-synthesis purification step. The copper(II) salts CuCl₂·2H₂O, Cu(OAc)₂·H₂O, Cu(acac)₂, Cu(NO₃)₂·3H₂O, CuSO₄·5H₂O were supplied by Merck and used as such. The solvents were purified before synthesis by standard procedure. The pyridine and dimethylsulfoxide (DMSO) used during the antimicrobial screening tests were sterilized before use.

2.2. Synthesis of ligand pyridoxal isonicotinoyl hydrazone (HL)

The ligand **HL** was prepared by refluxing an equimolar mixture of pyridoxal hydrochloride and isonicotinoyl hydrazide. The amount of pyridoxal hydrochloride (0.204 g, 1 mmol) was dissolved at room temperature in methanol (10 mL). Paralelly, the corresponding amount of isonicotinoyl hydrazide (0.137 g, 1 mmol) was dissolved in the same solvent (10 mL). The pale yellow mixture formed by the two methanolic solutions was refluxed for one hour. Afterwards, it was left to cool at room temperature. The resulting orange precipitate was filtered, washed with alcohol and dried in vacuum. In order to obtain the orange single crystals suitable for X-ray diffraction, a certain amount of solid ligand was re-dissolved in a mixture methanol:DMSO (3:1, v/v). After the slow evaporation of the obtained solution the single crystals were isolated and filtered.

Yield: 63%; M. wt: 322.5 g/mol; Anal. Calc. for $C_{14}H_{15}N_4O_3Cl$: C, 52.09; H, 4.65; N, 17.36; Cl, 11.00%. Found: C, 52.85, H, 4.30, N, 17.08, Cl, 10.57%. Main IR peaks (KBr, cm^{-1}): The condensation of the two reagents with the formation of the hydrazone **HL** is confirmed by the appearance in the IR spectrum of the signal at 1605 cm^{-1} . This signal is typical for the vibration of the azomethine bond [25,26]; $\nu(OH)$ 3595, 3247; $\nu(C=O)$ 1685; $\nu(C=N)$ 1605; $\nu(Ar-OH)$ 1267; $\nu(N-NH)$ 1093; $\nu(CH_2-OH)$ 1029. 1H NMR (DMSO- d_6 , δ (ppm), J (Hz)): The formation of the azomethine group is emphasized by the presence of the signal at δ 9.18 ppm in the 1H NMR spectrum. 2.63 (s, 3H, CH_3); 4.77 (s, 2H, CH_2-OH); 7.85 (d, 2H, H-2, H-6); 8.03 (d, 2H, H-3, H-5); 8.17 (s, 1H, OH); 8.86 (s, 1H, NH); 9.18 (s, 1H, $CH=N$). ^{13}C NMR (DMSO- d_6 , δ (ppm), J (Hz)): The presence of the imine fragment in the molecule of hydrazone **HL** is confirmed also by the signal registered at δ 149.94 ppm in the ^{13}C NMR spectrum. 38.66 (CH_3); 58.19 (C5); 122.00 (C6); 126.25 (C17, C21); 130.19 (C18, C20); 136.69 (C16); 149.94 ($HC=N$); 152.82 (C3); 161.68 (C=O).

Please insert **Scheme 1** here

2.3. Synthesis of the complexes

All the complexes have been synthesized by the direction reaction between ligand **HL** and each of the copper salts.

2.3.1. Synthesis of complex $[CuLCl(H_2O)_2]$ (**1**)

To a solution of ligand pyridoxal isonycotinoyl hydrazone (0.286 g, 1 mmol) in methanol (25 mL) was added a solution of $CuCl_2 \cdot 2H_2O$ (0.17 g, 1 mmol) in methanol (15 mL). The pH of the solution was adjusted by adding dropwise an alcoholic solution of NaOH. The mixture was refluxed for 3 hours. The dark green solid obtained was filtered, washed with alcohol and dried in vacuum. The complex is soluble in pyridine, slightly soluble in DMSO and insoluble in methanol and ethanol. Yield: 71%; M.wt.: 420.5 g/mol. Anal. calc. for $CuC_{14}H_{17}N_4O_5Cl$: C, 39.95; H, 4.04; N, 13.31; Cu, 15.21%. Found: C, 39.36; H, 4.32; N, 13.08; Cu, 15.36%. Main IR peaks (KBr, cm^{-1}): 3418, $\nu(OH)$; 1611, $\nu(C=O)$; 1583, $\nu(C=N)$; 1217, $\nu(Ar-OH)$; 1095, $\nu(N-NH)$; 1029, $\nu(CH_2-OH)$. μ_{eff} = 1.7.

2.3.2. Synthesis of complex $[CuL(OAc)](H_2O)$ (**2**)

A solution of $Cu(OAc)_2 \cdot H_2O$ (0.199 g, 1 mmol) in methanol (10 mL) was added to a warm solution of **HL** (0.286 g, 1 mmol) in methanol (10 mL). The mixture was refluxed for 3-4 hours. A solid brown precipitate was isolated and dried. Complex **2** is soluble in pyridine, slightly soluble in DMSO and DMF and insoluble in alcohols. Yield: 78%; M.wt.: 427 g/mol. Anal. calc. for $CuC_{16}H_{18}N_4O_6$: C, 44.96; H, 4.44; N, 13.11; Cu, 14.98%. Found: C, 45.31; H, 4.01; N, 12.25; Cu, 14.10%. Main IR peaks (KBr, cm^{-1}): 3349, $\nu(OH)$; 1606, $\nu(C=O)$; 1575, $\nu(C=N)$; 1207, $\nu(Ar-OH)$; 1097, $\nu(N-NH)$; 1030, $\nu(CH_2-OH)$. μ_{eff} = 1.5.

2.3.3. Synthesis of complex $[CuL(OAcac)]$ (**3**)

This complex was synthesized by refluxing a 1:1 mixture of ligand and copper(II) acetylacetonate. The $Cu(acac)_2$ (0.261 g, 1 mmol) was dissolved in a small volume of chloroform (5 mL) and resulting solution was added to a

methanolic solution of corresponding amount of ligand **HL** (0.286 g, 1 mmol). The mixture was heated at 50°C for 5 hours. Once the solution was left to cool at room temperature a brown solid compound was isolated, washed with a chloroform:methanol mixture and dried. The obtained complex is soluble in pyridine and slightly soluble in DMSO. Yield: 60%; M.wt.: 448 g/mol. Anal. calc. for $\text{CuC}_{19}\text{H}_{20}\text{N}_4\text{O}_5$: C, 50.89; H, 4.46; N, 12.50; Cu, 14.28%. Found: C, 51.25; H, 4.18; N, 11.37; Cu, 13.77%. Main IR peaks (KBr, cm^{-1}): 3324, $\nu(\text{OH})$; 1606, $\nu(\text{C}=\text{O})$; 1560, $\nu(\text{C}=\text{N})$; 1204, $\nu(\text{Ar-OH})$; 1092, $\nu(\text{N-NH})$; 1025, $\nu(\text{CH}_2\text{-OH})$. $\mu_{\text{eff}}=1.9$.

2.3.4. Synthesis of complex $[\text{CuL}(\text{NO}_3)](\text{H}_2\text{O})$ (**4**)

Complex **4** was prepared in a similar fashion as complex **2**. To a warm solution of ligand (0.286 g, 1 mmol) dissolved in methanol was slowly added a solution of $\text{Cu}(\text{NO}_3)_2 \cdot 3\text{H}_2\text{O}$ (0.241 g, 1 mmol). The resulting solution was heated under continuous stirring for 3 hours. A brown solid was obtained. Finally, it was filtered, washed with alcohol and dried. Complex **4** is soluble in pyridine and insoluble in alcohols, acetonitril or acetone. Yield: 85%; M. wt.: 430 g/mol. Anal. calc. for $\text{CuC}_{14}\text{H}_{15}\text{N}_5\text{O}_7$: C, 39.06; H, 3.48; N, 16.27; Cu, 14.88%. Found: C, 39.55; H, 3.02; N, 16.20; Cu, 14.49%. Main IR peaks (KBr, cm^{-1}): 3349, $\nu(\text{OH})$; 1606, $\nu(\text{C}=\text{O})$; 1575, $\nu(\text{C}=\text{N})$; 1207, $\nu(\text{Ar-OH})$; 1089, $\nu(\text{N-NH})$; 1030, $\nu(\text{CH}_2\text{-OH})$; 1090, $\nu(\text{O-NO}_2)$; 1280, 1430, $\nu(\text{NO}_3)$. $\mu_{\text{eff}}=1.6$.

2.3.5. Synthesis of complex $[\text{CuL}_2](\text{H}_2\text{O})$ (**5**)

Complex **5** was prepared by stirring at reflux temperature a 2:1 mixture of ligand **HL** (0.286 g, 1 mmol) and $\text{CuSO}_4 \cdot 5\text{H}_2\text{O}$ (0.249 g, 1 mmol). After one hour a solid green compound was obtained. The mixture was stirred for another 2 hours in order to increase the yield of complex formation. Afterwards, the obtained compound was filtered and dried. The novel complex is soluble in pyridine. Complex **5** is soluble in pyridine and insoluble in alcohols. Yield: 65%; M.wt.: 654. Anal. calc. for $\text{CuC}_{28}\text{H}_{28}\text{N}_8\text{O}_7$: C, 51.37; H, 4.28; N, 17.12; Cu, 9.78%. Found: C, 51.74; H, 3.96; N, 16.94; Cu, 9.63%. Main IR peaks (KBr, cm^{-1}): 3349, $\nu(\text{OH})$; 1606, $\nu(\text{C}=\text{O})$; 1575, $\nu(\text{C}=\text{N})$; 1207, $\nu(\text{Ar-OH})$; 1100, $\nu(\text{N-NH})$; 1030, $\nu(\text{CH}_2\text{-OH})$. $\mu_{\text{eff}}=1.8$.

Please insert **Scheme 2** here

2.4. Physical measurements

The percentages of C, H and N were determined by elemental analysis using a Carlo-Erba microdosimeter. The amount of copper(II) was determined by atomic absorption spectroscopy. The IR spectra were measured by using KBr pelletizing technique and registered with a BioRad FTS 135 spectrophotometer. The NMR results were obtained using a solution of ligand **HL** dissolved in DMSO; the spectra was recorded using a Bruker DRX 400 spectrometer. The electronic spectra were registered with a Jasco V-670 spectrophotometer using samples optically diluted with MgO. The X-band (9.2-9.6 GHz) EPR spectra were performed at room temperature on weighted microcrystalline powder samples, in the same conditions of modulation, amplitude and microwave power, using a CMS 4800 Adani EPR spectrometer (details in [27]). Spectra simulations were done with Bruker Simfonia and SIM

software. The magnetic susceptibility measurements were performed at 20°C on polycrystalline powders of all five complexes using a home-made Faraday magnetic balance. The thermal analysis studies were made by using certain amounts of samples in polycrystalline state. The analysis were conducted in nitrogen atmosphere by gradually increasing the temperature between 30°C-900°C with 10°C/minute. The analysis were conducted with a Perkin Elmer STA-600 thermal analyzer.

2.5. X-ray diffraction

Crystallographic measurements for the ligand **HL** were carried out with an Oxford-Diffraction XCALIBUR E CCD diffractometer equipped with graphite-monochromated Mo-K α radiation. Single crystals were positioned at 40 mm from the detector and 374 frames were measured each for 10 s over 1° scan width. The unit cell determination and data integration were carried out using the CrysAlis package of Oxford Diffraction [28a]. The structures were solved by direct methods using Olex2 [28b] software with the SHELXS structure solution program and refined by full-matrix least-squares method on F² with SHELXL-97 [28c]. Atomic displacements for non-hydrogen atoms were refined using an anisotropic model. Hydrogen atoms were placed in fixed, idealized positions and refined as rigidly bonded to the corresponding carbon atoms. Hydrogen atoms for NH and OH groups have been placed by Fourier Difference, accounting for the hybridization and the hydrogen bonds parameters. The molecular plots were obtained using the Olex2 program. The main crystallographic data data together with refinement details are summarized in Table 1, while the bond distances and angles in table 1S. The crystallographic measurements for complexes **1-5** were carried out on polycrystalline powders with a X-ray diffractometer Epyrean which uses a characteristic X-rays beam Cu K α_1 ($\lambda = 1.540598$). The diffractometer was equipped with a hybrid monochromator 2xGe(220) for Copper and a detector PIXcel3D. The analysis was made by applying the Bragg-Brentano geometry (“theta-2-theta”) for angles 2 θ between 5°-60°, with an increasing step of 0,04° and acquisition time per step of 500 seconds. A small amount of complex sample was positioned on a silica monocystal support. The complex polycrystalline sample was pressed on the support in order to obtain a thin, flat layer. The crystal system was identified by using the McMaille method, while the space group was determined the LeBail method, followed by structure refinement. The selection of the parameters for structures refinement was based on the “goodness of fit” (GOF) index. After the identification of crystal system and space group one additional step was to realize the fit profile by using the Pawley method. For the identification of all parameters it was considered that the each sample contains only one mineralogical phase.

Please insert **Table 1** here

2.6. Antimicrobial activity

The ligand **HL** and the corresponding Cu(II) complexes were tested in respect to their antimicrobial potential. We assessed the inhibition capacity of the ligand, solvents (pyridine and dimethylsulfoxide) and the five newly synthesized Cu(II) hydrazone complex compounds against *Escherichia coli* W3110, *Pseudomonas aeruginosa*

ATCC 9027 (Gram-positive) and *Bacillus cereus ATCC 14579*, *Staphylococcus aureus ATCC 6538* (Gram-negative) bacterial strains. As control drug two aminoglycoside antibiotics (streptomycin sulfate salt, kanamycin sulfate) and one beta-lactam antibiotic (ampicillin sodium salt) were used (all from Sigma- Aldrich). The minimal inhibitory concentrations (MIC) were determined by Mueller-Hinton Broth (MHB) microdilution method proposed by Wiegand et al. 2008 [29]. The MIC of ligand **HL** and complexes **1-5** were compared against the ones of the antibiotics used as standards. In order to determine the MIC ($\mu\text{g/mL}$) for ligand and complexes a stock solution with concentration 2048 $\mu\text{g/mL}$ was prepared by dissolving the appropriate amount of compound in a pyridine:DMSO (1:5, v/v) mixture. Further, by diluting the stock solution with the same solvents mixture was obtained a series of subsequent solutions with gradually decreasing concentrations: 1024, 512, 256, 128, 64, 32, 16, 8, 4, 2, 1, 0.5, 0.25, 0.125, 0.063, 0.03, 0.015 $\mu\text{g/mL}$. Other materials used for the quantitative screening were 96-well plates, suspension of microorganism (0.5 McFarland) and Muller-Hinton broth. After incubation at 37^oC for 24-48 hours of the inoculated plates, the MIC of all complexes against each microbial strain was determined by macroscopic observation.

3. Results and discussion

The hydrazone ligand **HL** was prepared by a condensation method which was used in our working group for the synthesis of other classes of compounds containing the azomethine group as well [30, 30a].

The new compound was obtained with a good yield and its molecular formula and structure were proven based on the results of the IR, ¹H and ¹³C RMN spectroscopy and elemental analysis. Moreover, based on the X-ray diffraction results the firstly reported structure of this hydrazone was obtained.

All the complexes were prepared by the direct reaction between the ligand **HL** and each of the copper(II) salts. Dark green and brown powders were obtained in significant yield (higher than 60%). The structures of the complexes were influenced by the ligand coordination capacity to the metal ion, the nature of the anionic groups and the working conditions. The results of the elemental analysis, spectral data and decomposition pattern confirm the predicted molecular formula. For complex **1** the formula [CuLCl(H₂O)₂] is proposed. Complexes **2** and **4** share a common general formula [CuLX](H₂O), where X=OAc⁻ (**2**) and X=NO₃⁻ (**4**). In case of complex **3** the IR spectra indicates the coordination of an acetylacetonate group to the Cu(II) ion confirming the formula [CuL(acac)]. Complex **5** is different than all the previous compounds of this class by having two molecules of ligand coordinated to a single copper ion – [CuCl₂](H₂O).

3.1. Crystal structure of ligand **HL**

As can be seen from Fig. 1, the crystal structure of the ligand comprises chlorhydrate units **H₄LCl** and DMSO as solvate molecules in 1:2 ratio. All the components of the structure are strongly associated via numerous O-H...Cl, O-H...N, O-H...Cl, N-H...Cl, N-H...O and C-H...O hydrogen bonding. The parameters of the hydrogen bonds are summarized in Table 2. Beside the above mentioned hydrogen bonding π - π stacking interactions are also observed in the packing of **H₄LCl**. It is realized through the Cg1 and Cg1' centroids of two centro-symmetrically related

C1/C2/C3/C4/N1/C5 rings, separated at 4.039 Å. The crystal structure motif of **H₄LCl** is characterized as the parallel packing of the column-like architecture, as shown in Fig. 2.

Please insert **Fig. 1** here

Please insert **Fig. 2** here

Please insert **Table 2** here

3.2. X-ray powder diffraction

The elemental cell parameters, crystallin system and spatial group for complexes **1-5** are presented in Table 2S. The crystallographic data indicate the same *triclinic* crystallin system for complexes **1** and **5** while in case of complexes **2** and **4** the *monoclinic* system is identified. Complex **4** is different than all the other compounds presenting a *hexagonal* crystallin system. Among the serie of complexes it can be observed similarities between the crystallin system and complexes geometries proposed based on the results of other techniques.

3.3. Infrared spectra and coordination mode

The assignment of the bands identified in the infrared spectra of the ligand and all complexes have been made based on the relevant literature materials [31]. In case of the complexes, the comparision of their infrared spectra with the spectra of ligand provided valuable information about the coordination mode to the copper ion. The main bands identified in the infrared spectra of the ligand and complexes are summarized in the *Experimental* section.

The condensation of the two reagents with the formation of the hydrazone ligand is proven by the presence of the band at 1605 cm⁻¹ in the spectra of ligand. This signal is specific to the imine streching frequency $\nu(\text{C}=\text{N})$ [5, 11a, 25]. Moreover, the absence of the bands characteristic to the carbonyl and amino groups indicates once again the formation of the proposed hydrazone. The presence of the hydroxyl group is emphasized by the sharp signals at 1267 cm⁻¹ ($\nu(\text{Ar-OH})$) and 1024 cm⁻¹ ($\nu(\text{CH}_2\text{-OH})$). Additionally, the infrared spectra exhibits a broad signal between 3250-3450 cm⁻¹ which is assigned to a hydrogen intramolecular bond ($\text{N}\cdots\text{OH}$) [10]. Due to the presence of $-\text{C}=\text{N}-\text{NH}-\text{C}=\text{O}$ group the ligand **HL** is potentially subject to keto-enol tautomerism (Scheme 3). The region between 1270-1690 cm⁻¹ in the IR spectra of the free ligand provides important information about the tautomeric form stabilized by the ligand molecule. The presence of the strong signal characteristic to the vibration of the C=O group and the lack of band assigned to $\nu(=\text{C-OH})$ in the spectra of the free ligand indicates that the hydrazone **HL** stabilizes the keto tautomeric form. The signal recorded at 1548 cm⁻¹ is the result of the coupled effect of the streching vibration mode of the N-C=O group and the NH bond deformation. The deformation mode $\delta(\text{NH})$ is also connected to the weak signal at 1315 cm⁻¹ [32]. These observations are confirmed also by the presence of the signal characteristic to the C=O signal in the ¹³C NMR spectra. Moreover, the X-ray diffraction analysis support the keto form proposed based on the spectral analysis.

A similar group of signals is emphasized in the infrared spectra of the copper complexes derived from the hydrazone **HL**. The signal specific to the vibration of the C=O group is clearly visible in the spectra of all complexes between

1606-1611 cm^{-1} indicating that the structure of the ligand does not undergo any structural change after coordinating to the metal ion. On the other hand, the band assigned to the carbonilic group is shifted to lower wavenumbers in the infrared spectra of all complexes compared to the spectra of free ligand. Such behaviour indicates that the oxygen atom of the C=O group is involved in the coordination. The band associated to the stretching vibration of the C=N group appears in the region 1546-1583 cm^{-1} in the spectra of complexes **1-5**. The negative shift by 22-59 cm^{-1} in the spectra of the complexes compared to the spectra of ligand suggest a decrease of the stretching force constant due to the coordination via the nitrogen atom of the azomethine bond [25]. In a similar manner, the band specific to the deformation vibration of Ar-OH group is moved from 1267 cm^{-1} in the spectra of ligand to 1230-1204 cm^{-1} in the spectra of complexes indicating that a third position in the coordination sphere is occupied by the oxygen atom of the deprotonated hydroxy group. The band associated to the second hydroxyl group (-CH₂-OH) does not undergo any change in respect to its position in the spectra of complexes compared to the spectra of **HL** thus suggesting that this fragment of the molecule is not involved into coordination. Therefore, it can be concluded that the hydrazone **HL** coordinated to the copper(II) ion in the keto form as a monobasic tridentate ligand, generating a five-atoms chelate ring and a six-atoms one. This finding is in accord with the behaviour of previously reported similar mononuclear hydrazone derived complexes [10, 11a, 33]. In case of complex **2** the vibrational spectra shows two bands at 1601 cm^{-1} and 1411 cm^{-1} . The position and the difference between these characteristic frequencies of these two signals suggest that the acetate anion participates to coordination as monodentate agent [31]. The IR spectra of complex **4** presents two additional signals at 1280 cm^{-1} and 1430 cm^{-1} associated to NO₃⁻ group. The difference between the frequencies of these signals $\Delta\nu=150 \text{ cm}^{-1}$ indicates a monodentate coordination manner of the nitro group [31,34]. A different pattern can be observed for complexes **1** and **5** in case of which the IR spectra do not show the specific signals associated to the coordinated chloride ion and sulphate ion, respectively. This is an indication that none of the mentioned anions participate into the coordination sphere of complexes **1** and **5**.

Please insert **Scheme 3** here

3.4. Electronic spectra and magnetic susceptibility

The electronic spectroscopy coupled with the results of magnetic susceptibility analysis was an effective method for the determination of the geometry of complexes. The electronic absorption spectra of ligand and complexes were recorded on polycrystalline samples diluted with an optically inactive matrix (MgO). The electronic spectra of the hydrazone **HL** exhibits one intense absorption band at 26.300 cm^{-1} with an additional shoulder at 22.200 cm^{-1} . These signals are assigned to the $n \rightarrow \pi^*$ and $\pi \rightarrow \pi^*$ transitions of the azomethine chromophore [35]. The broad and lower intensity band recorded in the region of the spectra below 38.000 cm^{-1} is specific to the transition associated to the pyridine moiety. In the spectra of the complexes the bands generated by the intraligand charge transfer are shifted to lower frequencies indicating the coordination of the hydrazone via the nitrogen atom of the azomethine bond. In addition, the complexes spectra display supplementary absorption bands specific to the d-d transitions. Complete data are provided in Table 3. The magnetic moments recorded at 20°C are characteristic to the system containing one unpaired spin and suggest that all complexes present paramagnetic properties (Table 3). This is also an evidence

of the mononuclear structure of all five complexes. The spectra of complexes **2** and **4** have a very similar layout, displaying a very wide band with absorption maxima between 15.100-15.800 cm^{-1} . Due to the strong dynamic Jahn-Teller effect the geometry of these complexes is significantly distorted [36a]. Consequently, the bands specific to the d-d transitions from the ground state ${}^2B_{1g}(d_{x^2-y^2})$ can be widened and overlapped resulting in a single broad signal. For these complexes the magnetic moments were determined between 1.5 – 1.6 MB. This is in accord with the previously reported and expected values for Cu(II) complexes in a distorted square-planar environment [36b]. The electronic spectra of complex **3** presents two well-defined bands with absorption maxima at 9.850 cm^{-1} and 15.130 cm^{-1} . These signals can be assigned to the d-d transitions ${}^2B_2 \rightarrow {}^2E(d_{xy} \rightarrow d_{xz, yz})$ and ${}^2B_2 \rightarrow B_1, {}^2A_1(d_{xy} \rightarrow d_{x^2-y^2}, z^2)$ which are typical for tetrahedral complexes [37]. In addition, the magnetic moment value (1.9 MB) confirms the proposed geometry and is also linked with the lower symmetry of the complex molecule. Complexes **1** and **5** are quite different than the others in respect to the layout of electronic spectra and magnetic susceptibility. The band with a maxima around 11.000 cm^{-1} is assigned to the transition ${}^2B_{1g} \rightarrow {}^2A_{1g}(d_{x^2-y^2} \rightarrow d_z^2)$. The next theoretically possible transition ${}^2B_{1g} \rightarrow B_{2g}(d_{x^2-y^2} \rightarrow d_{xy})$ is not visible, most probably being embedded by the wider band at lower frequency. The cause for this overlapping is connected with the very close energies of these two transitions and also with the Jahn-Teller distortion. The second observed band, higher in intensity, recorded around 15.000 cm^{-1} is typically associated to the transition ${}^2B_{1g} \rightarrow {}^2E_g(d_{x^2-y^2} \rightarrow d_{xz, yz})$. These data suggest a distorted octahedral geometry of these complexes and is in accord with previously reported observation for similar compounds [38]. Moreover, the magnetic moment values measured for these complexes (1.7 MB and 1.8 MB) are very similar to the one of 1.73 MB expected for a single unpaired spin confirming the octahedral geometry [39]. The proposed structures are supported by the EPR spectroscopy and thermal analysis as well.

Please insert **Table 3** here

3.5. EPR spectra

To correlate the above data with the local symmetry of copper in the complex lattice, EPR spectroscopy was used as a method-of-choice for its remarkable sensitivity and selectivity [40]. The room temperature EPR spectra recorded on the complexes **1** – **5** are presented in Fig. 3a. The main EPR feature of these spectra is their anisotropic line shape (of orthorhombic symmetry). The complexes **1** and **5** show an axial-like shape spectrum while the complexes **2**, **3** and **4** show only a single asymmetric broad line with different line width of 15.5 mT, 13.0 mT, and 14.1 mT, respectively. The main EPR parameters, g-tensor, were obtained by simulation of the experimental spectra. Figure 3b shows the EPR simulation spectra and their characteristic parameters are given in Table 4. It can be observed that the room temperature spectra do not reflect the static local configuration around Cu ion. It is well known the fluxionality of Cu complexes [41]. Such molecular motions can mediate the anisotropic parts of EPR spectra. Only low temperature measurements, at which molecular motions become frozen, can provide correct interaction tensors reflecting the static local configurations. A special comment can be although made for complexes **1** and **5**. Their EPR spectra (with $g_2 \approx g_3$) correspond approximately to an orthorhombic local symmetry. That suggests a more rigid

structure of the complexes, a conclusion in accordance with the proposed distorted octahedral coordination. Besides, the g-values of complexes **2** and **4** could imply a distorted square-planar geometry.

Please insert **Fig. 3** here

Please insert **Table 4** here

3.6. Thermal studies

In order to obtain further information about the thermal stability as well as the decomposition model we investigated the thermal behaviour of all complexes. For this purpose the TG, DTG and DTA curves were recorded by applying gradually increasing temperature to the polycrystalline samples of complexes. This technique has been proven very helpful especially in the determination of the small molecules presence. The results of the thermal analysis are presented in Table 5.

The general decomposition pattern describes few steps associated to the loss of smaller fragments (H_2O , Cl_2 , OAc^- , NO_3^-) as well as two mass loss recorded at high temperature generated by the decomposition of the ligand (overlapped in case of complexes **2**, **3** and **5**). TG curve for complex **1** describes two well defined steps associated to the loss of two water molecules (251-270 $^\circ\text{C}$) and one chloride (278-300 $^\circ\text{C}$). The sequence of these molecules loss as well as the loss temperature indicate that both the anion chloride and the H_2O molecules are involved in the coordination sphere. The thermal curves for complexes **2** and **4** are similar, indicating the exothermic elimination of one water molecule and one coordinated acetate anion (complex **2**) and nitrate anion (complex **4**) respectively. The low temperature at which the first decomposition process is observed demonstrates the crystallization nature of the water molecule [42]. Still, in case of complex **4** this process occurs at slightly higher temperature which suggests the involvement of crystallization water in intermolecular interactions [43]. For complex **3** the DTA and TG curves present three exothermic processes. The one at lowest temperature (278-300 $^\circ\text{C}$) corresponds to the elimination of the coordinated acetylacetonate fragment, while the overlapped ones occurring at higher temperatures (>530 $^\circ\text{C}$) describe the degradation of the ligand. The TG curve of complex **5** describes a mass loss at low temperature (50-97 $^\circ\text{C}$) associated to one molecule of crystallization water. Between 265-420 $^\circ\text{C}$ a significant mass loss occurs due to the loss of one of the two molecules of ligand. In case of all complexes the degradation processes lead to CuO formation.

Please insert **Table 5** here

3.7. Antimicrobial activity

The antimicrobial activity of the ligand **HL** and complexes **1-5** was tested against a spectrum of Gram-positive and Gram-negative bacteria. The minimal inhibitory concentrations (MICs) are indicated in Table 6. The five newly synthesized Cu(II) complexes showed significantly higher antimicrobial activity compared to the uncoordinated ligand **HL**. The value of the minimal inhibitory concentration (MIC) in case of complexes **1-5** varies between 64-128 $\mu\text{g/mL}$, the observed values being 8-16 times smaller than those observed in the case of the ligand (MIC: 1024 $\mu\text{g/mL}$). The observed values of the MICs for utilized solvents (pyridine and DMSO) is 1024 $\mu\text{g/mL}$, showing a

higher value than the amount of the used solvents in experiments. Thus the solvents had no influence on the MIC values obtained for ligand and Cu(II) complexes.

The increased antimicrobial potential of the complexes compared to the ligand can be explained in view of two major concepts. When entering in direct contact with the pathogen bacteria the Cu(II) compounds cause cell damage by membrane ruptures leading to loss of membrane potential and cytoplasmic content. So they inhibit the growth of bacteria ultimately causing their death [44]. On the other hand, the chelation theory by Tweedy [45] as well as the theory of Searl [46] can be considered relevant to explain the enhanced microbiological effect of the complexes.

The obtained results are in accord with similar microbiology studies for other hydrazones. Previously, Angelusiu et al. evaluated the *in vitro* antibacterial effect of some aroyl-hydrazones and their Cu(II), Co(II) and Ni(II) complexes against Gram-positive bacteria (*Staphylococcus aureus*, *Bacillus subtilis*) and Gram-negative bacteria (*Pseudomonas aeruginosa*, *Escherichia coli*), using MICs method. The obtained results showed that the ligand had a weak action on all the tested microorganisms while the activity become more pronounced when coordinated to the metal ions [47]. The values of the MIC varied between 32-512 µg/mL (Angelusiu et al.), being higher than those observed by us in case of complexes **1-5**. Also, Özmen and Olgun demonstrated that sulfonyl hydrazone derivatives and their nickel complexes were exhibited antibacterial activity against Gram-positive bacteria (*Staphylococcus aureus*, *Bacillus megaterium*, *Bacillus subtilis*) and Gram-negative bacteria (*Salmonella enteritidis*, *Escherichia coli*) and possess broad spectrum of activity [48]. The MIC values varied between 145 and 683µg/mL (Özmen and Olgun), those compounds having an inferior antimicrobial capacity than the complexes described in the present study.

The inhibitory potential of ligand **HL** and complexes **1-5** was evaluated comparatively with the effect of three antibiotics currently used in therapy. In the study of the antimicrobial effect of the control drugs the most sensible bacterial strain was *E. coli* W3110 showing MIC values of 1 µg/mL for kanamycin, 2 µg/mL for ampicillin and 1 µg/mL for streptomycin. The next bacterial strain regarding the susceptibility was the *S. aureus* ATCC 6538 strain with the observed MIC values of 0.5-32 µg/mL. The smallest antimicrobial susceptibility were observed in case of *B. cereus* ATCC 14579 (MIC values 8-64 µg/mL) and *P. aeruginosa* ATCC 9027 (MIC values 256-1024 µg/mL) bacterial strains. In our study both *B. cereus* ATCC 14579 and *P. aeruginosa* ATCC 9027 bacterial strains showed ampicillin resistance. *P. aeruginosa* is often resistant to multiple antibiotics and consequently has joined the ranks of 'superbugs' due to its enormous capacity to engender resistance. Compared with other pathogens, *P. aeruginosa* is very difficult to eradicate as it displays high intrinsic resistance to a wide variety of antibiotics, including aminoglycosides, fluoroquinolones and β-lactams [49]. In case of the four studied bacterial species strains showing a broad spectrum of resistance against antibiotics was observed [50-53]. On the other hand, it was observed that complexes **1**, **2** and **4** present a good inhibitory effect against *B. cereus* ATCC 14579 and *P. aeruginosa* ATCC 9027 bacterial strains their MIC values (64 µg/mL) being 8 times lower than the MIC of ampicillin and streptomycin. In view of these results, the presented Cu(II) complexes can be considered an important alternative class of compounds for new drug development.

Please insert **Table 6** here

4. Conclusion

In order to develop new effective antimicrobial agents we synthesized and structurally characterized five Cu(II) complexes with the ligand obtained by condensation of pyridoxal hydrochloride and isonicotinoyl hydrazide (HL). The physico-chemical data confirm the molecular structure of compound **HL** while the stereochemistry of the complex **1-5** was proposed based on IR, UV-VIS, EPR spectroscopy and magnetic moments values. The nature and number of additionally coordinated small fragments as well as the thermal stability were determined by analyzing the TG, DTG and DTA curves. In case of all chelate compounds, **HL** acts as tridentate monoanionic ligand keeping the same keto tautomeric form as prior coordination. The effect of the contraction from the Cu(II) salts is clearly observed. For complexes **1** and **5** the spectral data indicate an octahedral geometry meanwhile compounds **2** and **4** adopts a square-planar surrounding of the Cu(II) ion. Complex **3** presents a lower-symmetry tetrahedral stereochemistry.

The single crystal X-ray diffraction data for **HL** show several intermolecular interactions via hydrogen bonds between ligand and neighboring HCl and DMSO molecules. In addition, the π - π stacking interactions between aromatic rings strengthen the resulting supramolecular structure.

The antimicrobial effect against *E. coli* W3110, *P. aeruginosa* ATCC 9027, *B. cereus* ATCC 14579 and *S. aureus* ATCC 6538 strains was tested from qualitative and quantitative perspective. Although the ligand had a low effect on the tested pathogen microorganisms the MIC values for complexes indicate up to 16 time increased antibacterial activity after coordination. This behaviour underlines the influence of the Cu(II) ion and the structure of complex molecules on the microbiological potential. The complexes are characterized by a wide antimicrobial spectrum exerting inhibitory effect against both Gram-positive and Gram-negative bacteria.

The activity of complexes **1-5** was compared with the one of other reference antibiotics. While *B. cereus* ATCC 14579 and *P. aeruginosa* ATCC 9027 can be considered resistant to ampicillin and streptomycin the complexes **1**, **2** and **4** were able to inhibit their growth at concentration of 64 μ g/mL. In view of these results, the presented Cu(II) complexes can be considered an important potential alternative class of compounds for new antimicrobial agents development.

Appendix A. Supplementary data

CCDC 934828 contains the supplementary crystallographic data for $C_{18}H_{27}ClN_4O_5S_2$ (HL). These data can be obtained free of charge via <http://www.ccdc.cam.ac.uk/conts/retrieving.html>, or from the Cambridge Crystallographic Data Centre, 12 Union Road, Cambridge CB2 1EZ, UK; fax: (+44) 1223-336-033; or e-mail: deposit@ccdc.cam.ac.uk.

Acknowledgements

The authors thank the Organic Chemistry Department, ICECHIM Bucharest (Romania) for microanalysis and Faculty of Technical and Social Sciences, Sapiientia Hungarian University of Transylvania (Romania) for

antimicrobial activity. This research was financially supported by European Regional Development Fund, Sectorial Operational Program „Increase of Economic Competitiveness”, Priority Axis 2 (SOP IEC-A2-O2.1.2-2009-2, ID 570, COD SMIS-CSNR:12473, Contract 129/2010-POLISILMET.

ACCEPTED MANUSCRIPT

References

- [1] (a) C.M. Armstrong, P.V. Bernhardt, P. Chin, D.R. Richardson, *Eur. J. Inorg. Chem.* 6 (2003) 1145;
- (b) J.R. Anacona, M. Rincones, *Spectrochimica Acta A* 141 (2015) 169;
- (c) E.N. Nfor, A. Husian, F. Majoumo-Mbe, I.N. Njah, O.E. Offiong, S.A. Bourne, *Polyhedron* 63 (2013) 207;
- [2] P. Vicini, M. Incerti, I.A. Doytchinova, P. La Colla, B. Busonera, R. Loddo, *Eur. J. Med. Chem.* 41 (2006) 624;
- [3] S. Rollas, S.G. Kucukguzel, *Molecules* 12 (2007) 1910;
- [4] A.A. Recio Despaigne, J.G. da Silva, A. C.M. do Carmo, F. Sives, O.E. Piro, E.E. Castellano, H. Beraldo, *Polyhedron* 28 (2009) 3797;
- [5] N.A. Mangalam, S. Sivakumar, M.R. Prathapachandra Kurup, E. Suresh, *Spectrochimica Acta A* 75 (2010) 686;
- [6] O. Pournalimardan, A.C. Chamayou, C. Janiak, H. Hosseini-Monfared, *Inorg. Chim. Acta* 360 (2007) 1599;
- [7] C. Basu, S. Chowdhury, R. Banerjee, H.S. Evans, S. Mukherjee, *Polyhedron* 26 (2007) 3617;
- [8] M. Bakir, O. Green, W.H. Mulder, *J. Mol. Struct.* 873 (2008) 17;
- [9] O.A. El-Gammal, G.A. El-Reash, S.F. Ahmed, *J. Mol. Struct.* 1007 (2012) 1;
- [10] H. Hosseini-Monfared, H. Falakian, R. Bikas, P. Mayer, *Inor. Chim. Acta* 394 (2013) 526;
- [11] (a) K.S. Abou-Melha, *Spectrochimica Acta A* 70 (2008) 162;
- (b) H.N. Fox, *Science* 116 (1952) 129;
- (c) J.R. Dilworth, *Coord. Chem. Rev.* 21 (1976) 29;
- [12] (a). S. Kakimoto, K. Yashamoto, *Pharm. Bull.* 4 (1956) 4;
- (b). V.J. Negi, A.Q. Sharma, J.S. Negi, V. Ram. *Int. J. Pharm. Chem.* 2 (2012) 100;
- (c). M. Asif. *Int. J. Adv. Chem.* 2 (2014) 85;
- [13] (a) G. Durgaprasad, C.C. Patel, *Indian J. Chem.* 11A (1973) 1300;
- (b) F. Martins, S. Santos, C. Ventura, R. Elvas-Leitao, L. Santos, S. Vitorino, M. Reis, V. Miranda, H.F. Correia, J. Aires-de-Sousa, V. Kovalishyn, D. A.R.S.Latino, J. Ramos, M. Viveiros, *Eur. J. Med. Chem.* 81 (2014) 119;

(c) E. Mackova, K. Hruskova, P. Bendova, A. Vavrova, H. Jansova, P. Haskova, P. Kovarikova, K. Vavrova, T. Simunek, *Chem-Biol. Interact.* 197 (2012) 69;

[14] R.K. Agarwal, D. Sharma, L. Singh, H. Argawal, *Bioorg. Chem. Appl.* (2006) 1;

[15] F.R. Pavan, P.I. da S. Maia, S.R.A. Leite, V.M. Deflon, A.A. Batista, D.N. Sato, S.G. Franzblau, C.Q.F. Leite, *Eur. J. Med. Chem.* 45 (2010) 1898;

[16] J.S. Casas, M.D. Couce, J. Sordo, *Coord. Chem. Rev.* 256 (2012) 3036;

[17] R. Chumnantana, N. Yokochi, T. Yagi, *Biochim. Biophys. Acta* 1722 (2005) 84;

[18] M. Adrover, B. Vilanova, F. Munoz, J. Donoso, *Bioorg. Chem.* 37 (2009) 26;

[19] S. Mann, O. Ploux, *Biochim. Biophys. Acta* 1814 (2011) 1459;

[20] H. Ota, M. Mushiga, T. Yoshimura, K. Yoshimune, *J. Biosci. Bioeng.* 120 (2015) 117;

[21] V.M. Leovac, M.D. Joksovic, V. Divjaskovic, L.S. Jovanovic, Z. Saranovic, A. Pevec, *J. Inorg. Biochem.* 101 (2007) 1094;

[22] M.S. Iqbal, A.H. Khan, B.A. Loothar, I.H. Bukhari, *Med. Chem. Res.* 18 (2009) 31;

[23] J.L. Buss, J. Neuzil, P. Ponka, *Biochem. Soc. T.* 30 (2002) 755;

[24] (a) J.P. Souron, M. Quarton, F. Robert, A. Lyubchova, A. Cosse-Barbi, J.P. Doucet, *Acta Crystallog. C* 51 (1995), 2179;

(b) M.R. Maurya, S. Agarwal, C. Bader, D. Rehder, *Eur. J. Inorg. Chem.* 147 (2005);

[25] K. Nakamoto, *Infrared Spectra of Inorganic and Coordination Compounds*, 5th edition, Wiley-Interscience, New York, 1997;

[26] S. Naskar, S. Naskar, R.J. Butcher, S.K. Chattopadhyay, *Inorg. Chim. Acta* 363 (2010) 404;

[27] F. Patrascu, M. Badea, M.N. Grecu, N. Stanica, L. Marutescu, D. Marinescu, C. Spinu, C. Tigae, R. Olar, *J. Therm. Anal. Calorim.* 113 (2013) 1421;

[28] (a) CrysAlis RED, Oxford Diffraction Ltd., Version 1.171.36.32, 2003 ;

(b) O.V. Dolomanov, L.J. Bourhis; R.J. Gildea, J. Howard, A. K. H. Puschmann, OLEX2: a complete structure solution, refinement and analysis program. *J. Appl. Cryst.* 42 (2009) 339;

(c) G.M. Sheldrick, SHELXS, *Acta Cryst.* **A64** (2008) 112;

- [29] I. Wiegand, K. Hilpert, E.W.R. Hancock, *Nat. Protoc.* 3 (2008) 163;
- [30] (a) T. Rosu, S. Pasculescu, V. Lazar, C. Chifiriuc, C. Cernat, *Molecules* 11 (2006) 904;
- (b) T. Rosu, E. Pahontu, R.S. Mezey, D.C. Ilies, R. Georgescu, S. Shova, A. Gulea, *Polyhedron* 31 (2012) 252;
- [31] K. Nakamoto, *Infrared and Raman Spectra of Inorganic and Coordination Compounds*, Wiley and Sons, New York 1986;
- [32] N. Galic, I. Brodanac, D. Kontrec, S. Miljanic, *Spectrochim. Acta A* 107 (2013) 263;
- [33] N. Galic, M. Rubcic, K. Magdic, M. Cindric, V. Tomisic, *Inorg. Chim. Acta* 366 (2011) 98;
- [34] N.F.Curtis, Y.M.Curtis, *Inorg. Chemistry* 4 (1965) 804;
- [35] A. Sreekanth, S. Sivakumar, M.R.P. Kurup, *J. Mol. Struct.* 655 (2003) 47;
- [36] (a) R. Selwin Joseyphus, M. Sivasankaran Nair, *Arabian J. Chem.* 3 (2010) 195;
- (b) D. Banerjea, *Coordination Chemistry*, Tata McGrwo-Hill Publisher, 1993;
- [37] A.B.P. Lever, *Inorganic Electronic Spectroscopy*, 2nd ed. Elsevier Science, New York, 1984;
- [38] R.B. Sumathi, M.B. Halli, *Bioinorg. Chem. Appl.* 2014 (2014);
- [39] D.W. Smith, *Inorg. Chem.* 5 (1966) 2236;
- [40] A. Lund, M. Shiotani, S. Shimada, *Principles and Applications of ESR Spectroscopy*, Springer Ed. 2011;
- [41] C.C. Chou, H.J. Liu, L.H.C. Chao, H.B. Syu, T.S. Kuo, *Polyhedron* 37 (2012) 60;
- [42] F. Patrascu, M. Badea, M.N. Grecu, N. Stanica, L. Marutescu, D. Marinescu, C. Spinu, C. Tigae, R. Olar, J. *Therm. Anal. Calorim.* 113 (2013) 1421;
- [43] D.B. Ninkovic, G.V. Janjic, S.D. Zaric. *Cryst. Growth Des.* 12 (2012) 1060;
- [44] G. Grass, C. Rensing, M. Solioz. *Appl. Environ. Microb.* 77 (2011) 1541;
- [45] B.G. Tweedy, *Phytopathology* 55 (1964) 910;
- [46] J.W. Searl, R.C. Smith, S.J. Wyard, *Proc. Phys. Soc.* 78 (1961) 1174;
- [47] M.V. Angelusiu, S.F. Barbuceanu, C. Draghici, G.L. Almajan. *Eur. J. Med. Chem.* 45 (2010) 2055;
- [48] U.Ol. Ozmen, G. Olgun. *Spectrochim. Acta A* 70 (2008) 641;
- [49] E.B. Breidenstein, C. de la Fuente-Nunez, R.E. Hancock. *Trends Microbiol.* 19 (2011) 419;

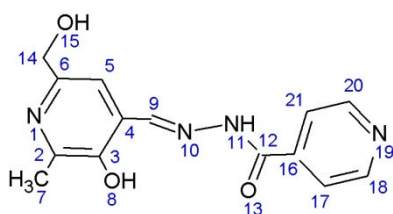
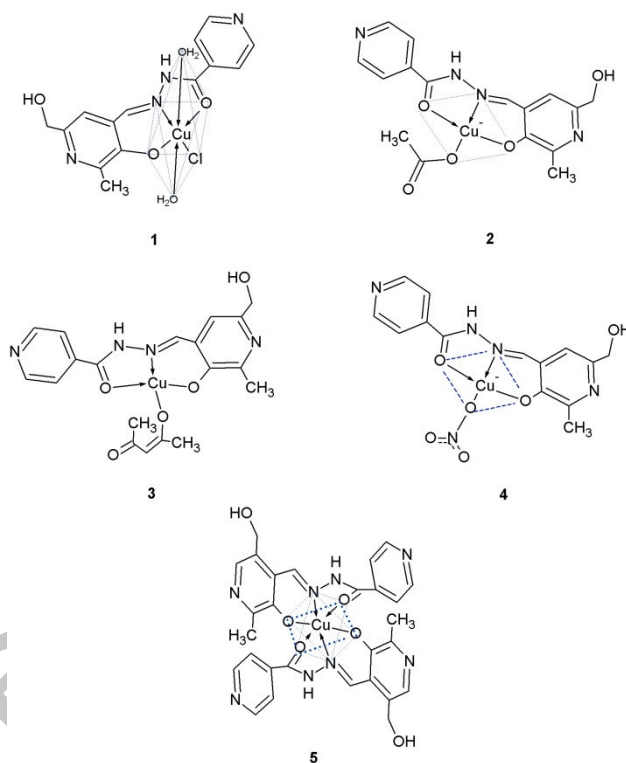
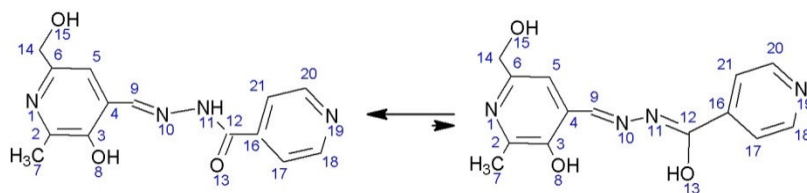
[50] L.B. Jensen, S. Baloda, M. Boye, F.M. Aarestrup. *Environ. Int.* 26 (2001) 581;

[51] G.G. Zhanel, T.L. Hisanaga, N.M. Laing, M.R. DeCorby, K.A. Nichol, B. Weshnoweski, J. Johnson, A. Noreddin, D.E. Low, J.A. Karlowsky. *Int. J. Antimicrob. Ag.* 27 (2006) 468;

[52] H.F. Chambers, F. DeLeo. *Nat. Rev. Microbiol.* 7 (2009) 629;

[53] R.J. Anderson, P.W. Groundwater, A. Todd, A.J. Worsley. Wiley & Sons, Ltd. United Kingdom (2012);

Figures and Tables

Scheme 1. Ligand pyridoxal isonicotinoyl hydrazone (**HL**)Scheme 2. Proposed structures for complexes **1-5**Scheme 3. Tautomeric equilibrium for ligand **HL**

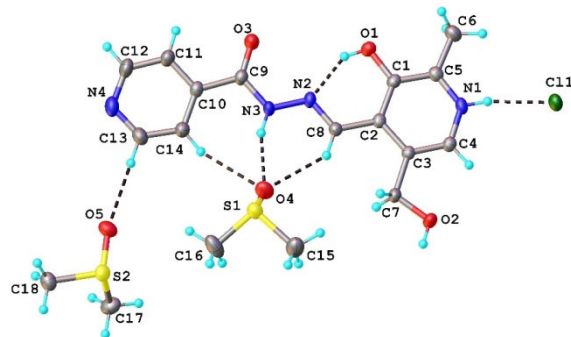


Fig. 1. View of the asymmetric part in the crystal structure H_4LCl , with thermal ellipsoids at 50% probability level.

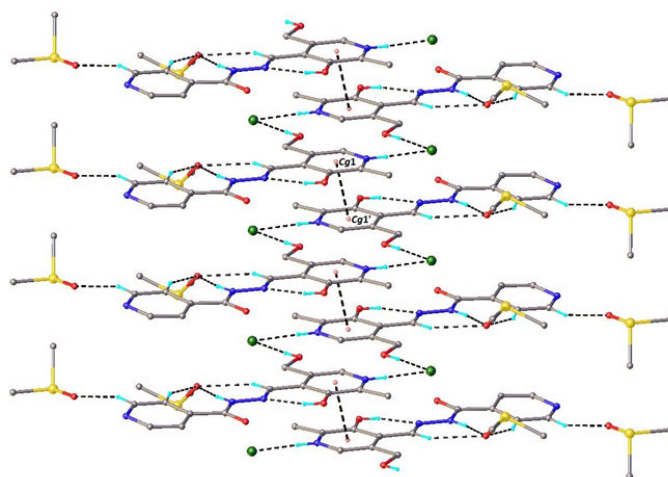


Fig. 2. The column-like supramolecular architecture in the crystal structure of H_4LCl .

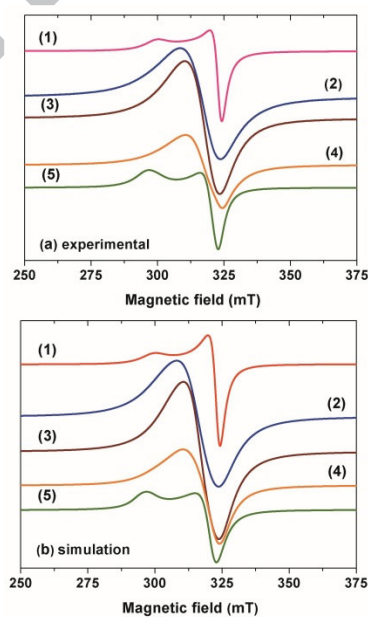


Fig. 3. EPR experimental spectra (a) and simulation spectra (b) for complexes **1-5**

Table 1. Crystallographic data, details of data collection and structure refinement parameters for ligand **HL**.

Empirical formula	C ₁₈ H ₂₇ ClN ₄ O ₅ S ₂
Formula weight	479.01
Temperature/K	200
Crystal system	triclinic
Space group	<i>P</i> -1
<i>a</i> /Å	5.9740(5)
<i>b</i> /Å	13.1953(19)
<i>c</i> /Å	15.3609(18)
<i>α</i> /°	71.755(12)
<i>β</i> /°	86.141(8)
<i>γ</i> /°	84.047(9)
<i>V</i> /Å ³	1143.0(2)
<i>Z</i>	2
<i>D</i> _{calc} /mg/mm ³	1.392
<i>μ</i> /mm ⁻¹	0.386
Crystal size/mm ³	0.30 × 0.15 × 0.15
<i>θ</i> _{min} , <i>θ</i> _{max} (°)	4.9 to 52.74
Reflections collected	8318
Independent reflections	4677 [<i>R</i> _{int} = 0.0261]
Data/restraints/parameters	4677/0/278
<i>R</i> ₁ ^a (<i>I</i> > 2σ(<i>I</i>))	0.0447
<i>wR</i> ₂ ^b (all data)	0.1019
GOF ^c	1.043
Largest diff. peak/hole/e Å ⁻³	0.25/-0.31

^a $R_1 = \sum ||F_o| - |F_c|| / \sum |F_o|$.

^b $wR_2 = \{ \sum [w (F_o - F_c)^2] / \sum [w (F_o)^2] \}^{1/2}$.

^c GOF = $\{ \sum [w (F_o - F_c)^2] / (n - p) \}^{1/2}$, where *n* is the number of reflections and *p* is the total number of parameters refined.

Table 2. Characteristics of hydrogen bonds

D–H···A	D–H	Distance, Å		DHA angle, deg	Symmetry code for A
		H···A	D···A		
O2–H···Cl1	0.82	2.24	3.053(2)	172.7	-1 - <i>x</i> , -2 - <i>y</i> , 2 - <i>z</i>
N3–H···O4	0.86	1.95	2.770(2)	158.8	<i>x</i> , <i>y</i> , <i>z</i>
N1–H···Cl1	0.86	2.20	3.048(2)	168.6	<i>x</i> , <i>y</i> , <i>z</i>
O1–H···N2	0.82	1.86	2.574(2)	145.5	<i>x</i> , <i>y</i> , <i>z</i>
C8–H···O4	0.93	2.37	3.139(2)	139.7	<i>x</i> , <i>y</i> , <i>z</i>
C14–H···O4	0.93	2.49	3.377(3)	158.4	<i>x</i> , <i>y</i> , <i>z</i>
C13–H···O5	0.93	2.56	3.452(3)	160.2	<i>x</i> , <i>y</i> , <i>z</i>

Table 3. Electronic spectra and magnetic moments for complexes **1-5**

Complex	Transitions d-d (cm^{-1})			$\mu_{\text{eff B.M.}}$	Geometry
[CuLCl(H ₂ O) ₂] (1)	$d_{x^2-y^2} \rightarrow d_z^2$ 11.840	$d_{x^2-y^2} \rightarrow d_{xy}$ -	$d_{x^2-y^2} \rightarrow d_{xz, yz}$ 15.400	1.7	Octahedral
[CuL(OAc)](H ₂ O) (2)	$d_{x^2-y^2} \rightarrow d_{xy}$ -	$d_{x^2-y^2} \rightarrow d_{yz, xz}$ 15.100		1.5	Square-planar
[CuL(OAcac)] (3)	$d_{xy} \rightarrow d_{xz, yz}$ 9.850	$d_{xy} \rightarrow d_{x^2-y^2}$ 15.130	$d_{xy} \rightarrow d_z^2$ -	1.9	Tetrahedral
[CuL(NO ₃)](H ₂ O) (4)	$d_{x^2-y^2} \rightarrow d_{xy}$ -	$d_{x^2-y^2} \rightarrow d_{yz, xz}$ 15.750		1.6	Square-planar
[CuL ₂](H ₂ O) (5)	$d_{x^2-y^2} \rightarrow d_z^2$ 11.560	$d_{x^2-y^2} \rightarrow d_{xy}$ -	$d_{x^2-y^2} \rightarrow d_{xz, yz}$ 14.920	1.8	Octahedral

Table 4. Principal values of g-tensor for complexes **1-5**

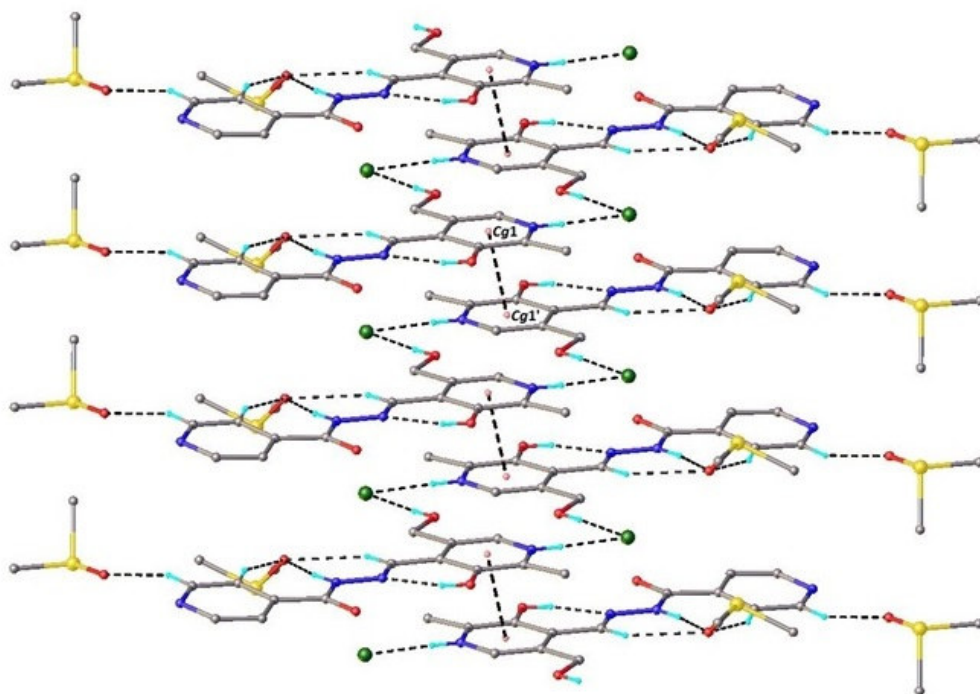
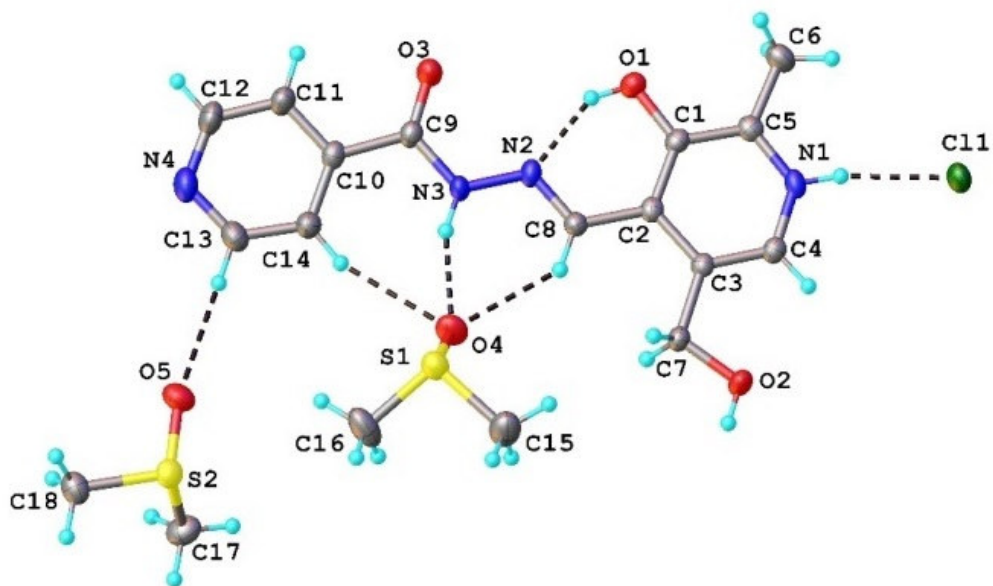
Complex	g_1	g_2	g_3
1	2.211	2.051	2.045
2	2.170	2.105	2.043
3	2.152	2.093	2.044
4	2.143	2.113	2.048
5	2.235	2.068	2.052
Errors:	± 0.003	± 0.003	± 0.003

Table 5. Thermal analysis data for complexes **1-5**

Complex	Temperature	Δm	Fragment lost
[CuLCl(H ₂ O) ₂] (1)	244-262°C	8.27%	2·H ₂ O
	279-294°C	9.21%	Cl ₂
	433-593°C		Ligand decomposition
[CuL(OAc)](H ₂ O) (2)	58-100°C	4.90%	H ₂ O
	270-330°C	13.36%	OAc ⁻
	554-607°C		Ligand decomposition
[CuL(OAcac)] (3)	231-353°C	22.32%	Acac ⁻
	534-615°C		Ligand decomposition
[CuL(NO ₃)](H ₂ O) (4)	70-105°C	4.97%	H ₂ O
	258-343°C	12.96%	NO ₃ ⁻
	524-601°C		Ligand decomposition
[CuL ₂](H ₂ O) (5)	50-97°C	2.80%	H ₂ O
	265-420°C	43.73%	Ligand
	433-582°C		Ligand decomposition

Table 6. MIC ($\mu\text{g/mL}$) values determined for ligand **HL**, complexes **1-5** and standard antibiotics

Compound	<i>Staphylococcus aureus</i> var. Oxford ATCC 6538	<i>Bacillus cereus</i> ATCC 14579	<i>Pseudomonas</i> <i>aeruginosa</i> ATCC 9027	<i>Escherichia coli</i> W3110
HL	1024	1024	1024	1024
[CuLCl] (1)	64	64	64	128
[CuL(OAc)](H ₂ O) (2)	64	64	64	128
[CuL(OAcac)] (3)	64	64	128	128
[CuL(NO ₃)](H ₂ O) (4)	64	64	64	128
[CuL ₂](H ₂ O) (5)	128	128	128	128
Ampicillin	0.5	resistant	resistant	2
Kanamycin	4	8	256	1
Streptomycin	32	64	256	1
Pyridine	1024	1024	1024	1024
DMSO	1024	1024	1024	1024



AC

The characterization of pyridoxal isonicotinoyl hydrazone (**HL**) and its Cu(II) complexes was done by ^1H NMR, ^{13}C NMR, UV–Vis, IR and EPR spectroscopy, thermal studies and elemental analysis. The structure of **HL** was determined by single crystal X-ray diffraction. The microbiological effect of ligand and complexes against Gram-positive and Gram-negative strains was tested.

ACCEPTED MANUSCRIPT